Hindawi
Mathematical Problems in Engineering
Volume 2020, Article ID 3197395, 19 pages
https://doi.org/10.1155/2020/3197395

Research Article

Dimensional and Layout Optimization Design of Multistage Gear Drives Using Genetic Algorithms

Lin Han, Geng Liu, Xiaohui Yang, and Bing Han

Shaanxi Engineering Laboratory for Transmissions and Controls, Northwestern Polytechnical University, Xi'an 710072, China

Correspondence should be addressed to Geng Liu; npuliug@nwpu.edu.cn

Received 17 May 2019; Accepted 14 January 2020; Published 31 January 2020

Academic Editor: Gustavo Scaglia

In the minimal weight/volume design of multistage gear drives, both the dimensional and layout parameters of gear pairs have a direct effect on the design result. A new optimization model that can carry out both dimensional- and layout-constrained optimization design for any number of stages of cylindrical gear drives simultaneously is proposed. The optimization design of a three-stage cylindrical gear drive is conducted as a design example to test the application of this model. In the attempt to solve this constrained optimization problem using an elitist genetic algorithm (GA), different constraint handling methods have a crucial effect on the optimal results. Thus, the results obtained by applying three typical constraint handling methods in GA one by one are analyzed and compared to figure out which one performs the best and find the optimal solution. Moreover, a more precise projection center distance (PCD) method to calculate the degree of interference constraint violation is proposed and compared with the usually used (0, 1) method. The results show that the proposed PCD method is a better one.

1. Introduction

The desire for designing multistage gear drives (MSGD) has been increased with the increasing need of high-speed-reduction ratio gear drives. Different from a single gear pair design, the tasks of MSGD design include the decision of transmission stages, the dimensional design of gear drive elements, and how to lay out them properly while satisfying various spatial constraints [1, 2]. All of these tasks are coupled with each other and involve numerous nonlinear formulations and various types of coefficients and variables based on recommended gear standards during the design process. It makes conventional trial and error methods a very complex and time-consuming activity and often ends up with a suboptimal or inadequate solution [3, 4].

The optimal design can be seen as a systematic or automatic design method for its ability to integrate the whole design process all in one with the aid of evolutionary algorithms. Meanwhile, an approximately optimal solution can be achieved, that is why optimal design methodology has been more and more widely used in gear drives design, especially during the preliminary design stage [5, 6]. Now, most of researchers focused their studies on dimensional optimization design problem that also called the minimal weight/volume design problem of gear drives. Yokota et al. formulated an optimal weight design problem of gear drive for a constrained bending strength of gear, torsion strength of shafts, and each gear dimension as a nonlinear integer programming (NIP) problem and then solved it by genetic algorithms (GAs) [7]. Savsani et al. employed particle swarm optimization, simulated annealing algorithms to solve the same optimization problem, and got some better results [8]. To obtain the optimal dimensions for gearbox, shaft, gear, and the optimal rolling bearing, Mendi et al. studied the dimensional optimization of motion and force transmitting components of a gearbox [9]. By choosing different values for the input power, gear ratio, and hardness of gears, Golabi et al. presented the practical graphs of optimization results. Through these graphs, all the necessary parameters of gearbox such as number of stages, modules, face width of gears, and shaft diameter can be derived [10]. The above research ignores the fact that the layouts including axis layout and orientation layout of gear drive components have a directly effect on the size of gearbox, and a proper layout can make the gearbox smaller and more compact. For instance, Figure 1 shows two possible axis layouts and orientation layouts of a three-stage gear drive and their effect on the size (i.e., length L_{Box}, width W_{Box}, and height H_{Box}) of gearbox. Chong et al. proposed a generalized methodology that contains four steps to integrate the dimensional and layout design process. In their study, the dimension and layout of gear components are obtained in separated steps, and these steps need to be iterated with each other to get the optimal dimension and layout of the gear components, which is a little bit complicated [11].

Therefore, the key issue of this paper is to propose and formulate an optimization model that can conduct the dimensional and layout optimization design of multistage cylindrical gear drives simultaneously. Comparing with other optimization methods, e.g., particle swarm optimization (PSO) method, the algorithmic process of genetic algorithm (GA) is a little complex. This is because GA needs variable encoding and genetic operators to transform the solution space of an actual problem into the searching space of GA. However, GA has been widely used in the optimization problem of gears and gearbox and proved itself to be working well and stable. Thus, GA was selected as the optimization method in this study. Furthermore, the objective in the optimization problem of this study is to minimize the overall volume of gear drives. The formulas of the proposed model are given in a general way so that they are applicable to any stages of cylindrical gear drive. The rest of this article is outlined as follows. Section 2 describes the formulas of design variables, objective function, and constraints. A proposed projection center distance (PCD) method to calculate the degree of the interference constraint violation is also introduced in this section. Section 3 describes some specific comments on the used elitism genetic algorithm (GA). In Section 4, the proposed optimization model is applied to the redesign task of a three-stage external spur gear drive, and a comparative analysis to the obtained optimization results is given. Some concluding remarks are made in Section 5.

2. Formulation of the Optimization Model

2.1. Design Variables. The design variables that are going to be optimized include two types of parameters of gear pairs and shafts: dimensional parameters that describe their basic geometry size and layout parameters that describe their position in three-dimensional space. The dimensional parameters consist of the number of teeth on pinion and wheels z_p, z_w, normal module m_n, face width coefficient ψ, and shaft diameter d_{sh}. The layout parameters consist of location parameter L and orientation parameter θ. The definitions of them are associated with the definition of global coordinate system (GCS). In this paper, the GCS, as shown in Figure 2, of a multistage gear drive is defined as follows: (I) the coordinate origin of GCS is located on the pinion axis of the first-stage gear pair; (II) the Y-axis of GCS is coaxial with the pinion axis of the first-stage gear pair; (III) the X-axis and Z-axis of GCS are parallel to the long edge and high edge of the gearbox, respectively, where the geometric shape of gearbox is assumed to be cuboid. Then, the location parameter L is defined as the distance between the pinion geometry center of a gear pair and the XOZ plane of GCS. In Figure 2, L_1 and L_2 are the location parameters of first-stage and second-stage gear pairs to the two-stage gear drive, respectively. Based on location parameters, the position of gear pairs on the shafts and the relative position of two gear pairs can be determined. The orientation parameter θ is defined as the angle at which the gear pair turns around its pinion axis. The range of θ is $[0^\circ, 360^\circ]$. When the value of θ equals 0° or 360°, the vector $\overrightarrow{O_{p,i}O_{w,i}}$ will be at the same direction with X-axis of GCS. Here, $O_{p,i}$ and $O_{w,i}$ are the geometry center of the i^{th}-stage gear pair's pinion and wheel, respectively. For instance, θ_1 and θ_2 in Figure 2 are the orientation parameters of first-stage and second-stage gear pairs.

Based on above statements, the design variables $\overrightarrow{x}$ to the dimensional and layout optimization design of an M-stage gear drive are

$$\overrightarrow{x} = \left\{z_{p,i}, z_{w,i}, m_{n,i}, \psi_i, L_i, \theta_i, d_{sh,j}\right\}, (i = 1, 2, \ldots, M; \quad j = 1, 2, \ldots, M + 1), \tag{1}$$

where M is a positive integer number that represents the number of stages of a gear drive. Thus, the number of design variables to an M-stage gear drive is $7M + 1$.

2.2. Objective Function. The minimization of the overall material volume of a gear drive, which is mainly made up by the material volume of gear pairs, shafts, and gearbox, is the optimization objective of this study. The formula of objective function for an M-stage gear drive is

$$F(\overrightarrow{x}) = \sum_{i=1}^{M} V_{\text{gearpair},i} + \sum_{j=1}^{M+1} V_{\text{shaft},j} + V_{\text{GearBox}}, \tag{2}$$

where

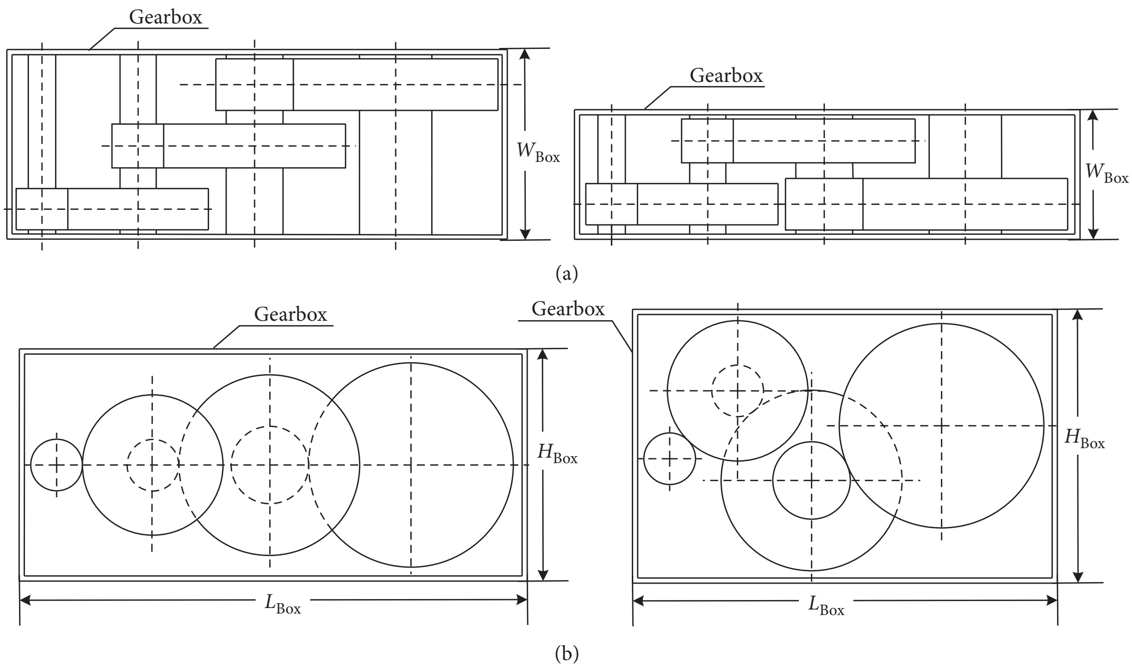

FIGURE 1: Two possible axis layouts and orientation layouts of a three-stage gear drive and their effect on the size of gearbox. (a) Two possible axis layouts of a three-stage gear drive and their effect on the width of gearbox. (b) Two possible orientation layouts of a three-stage gear drive and their effect on the length and height of gearbox.

$$\begin{cases} V_{\text{gearpair},i} = \dfrac{\pi B_i d_{p,i}^2}{4}\left(1+\left(z_{w,i}/z_{p,i}\right)^2\right) - \dfrac{\pi B_i}{4}\left(d_{sh,i}^2 + d_{sh,i+1}^2\right), \\ V_{\text{shaft},j} = \dfrac{\pi W_{\text{Box}}}{4} d_{sh,j}^2, \\ V_{\text{GearBox}} = L_{\text{Box}} W_{\text{Box}} H_{\text{Box}} - \left(L_{\text{net}} + 2\Delta_l\right)\left(W_{\text{net}} + 2\Delta_w\right)\left(H_{\text{net}} + 2\Delta_h\right), \\ (i = 1, 2, \ldots, M;\ j = 1, 2, \ldots, M+1), \end{cases} \tag{3}$$

where

$$\begin{cases} L_{\text{Box}} = L_{\text{net}} + 2\Delta_l + 2\Delta_t, \\ W_{\text{Box}} = W_{\text{net}} + 2\Delta_w + 2\Delta_t, \\ H_{\text{Box}} = H_{\text{net}} + 2\Delta_h + 2\Delta_t, \end{cases} \tag{4}$$

where $B_i = \psi_i d_{p,i}$ is the face width of i^{th}-stage gear pair, and $d_{p,i}$ is the pitch diameter of i^{th}-stage gear pair. L_{Box}, W_{Box}, and H_{Box} are the length, width, and height of gearbox, respectively, while L_{net}, W_{net}, and H_{net} are the length, width, and height of the bounding box (i.e., a box completely bounding the gear pairs, as shown in Figure 2), respectively. Furthermore, Δ_l, Δ_w, and Δ_h are the minimum gaps permitted for the bounding box and the inner wall of the gearbox in the length, width, and height directions, respectively. The values of them are set to 10 mm in this study. Δ_t is the thickness of the gearbox, and the value of it is set to 8 mm in this study.

Equation (4) reveals that the values of L_{Box}, W_{Box}, and H_{Box} are associated with the values of L_{net}, W_{net}, and H_{net}. The value of W_{net} can be easily calculated by the location parameter L_i and face width B_i of the i^{th}-stage gear pair. For instance, W_{net} of the two-stage gear drive in Figure 2 is $W_{\text{net}} = (L_1 + B_1/2) - (L_2 - B_2/2)$. To induce a formula to calculate the values of L_{net} and H_{net} for an M-stage gear drive, 8 edge-points $P_{i,k}$ $(k = 1, 2, \ldots, 8;\ i = 1, 2, \ldots, M)$ on the addendum circles of each gear pair are defined. Figure 3(a) displays the edge-points $P_{k,i}$ on the addendum circles of i^{th}-stage gear pair. An important character of the edge-points to the i^{th}-stage gear pair is that the lines $P_{i,3}P_{i,1}$ and $P_{i,7}P_{i,5}$ are always parallel to the X-axis of GCS, while the lines $P_{i,2}P_{i,4}$ and $P_{i,6}P_{i,8}$ are always parallel to the Z-axis of GCS, whatever the value of θ_i is. In an M-stage gear drive,

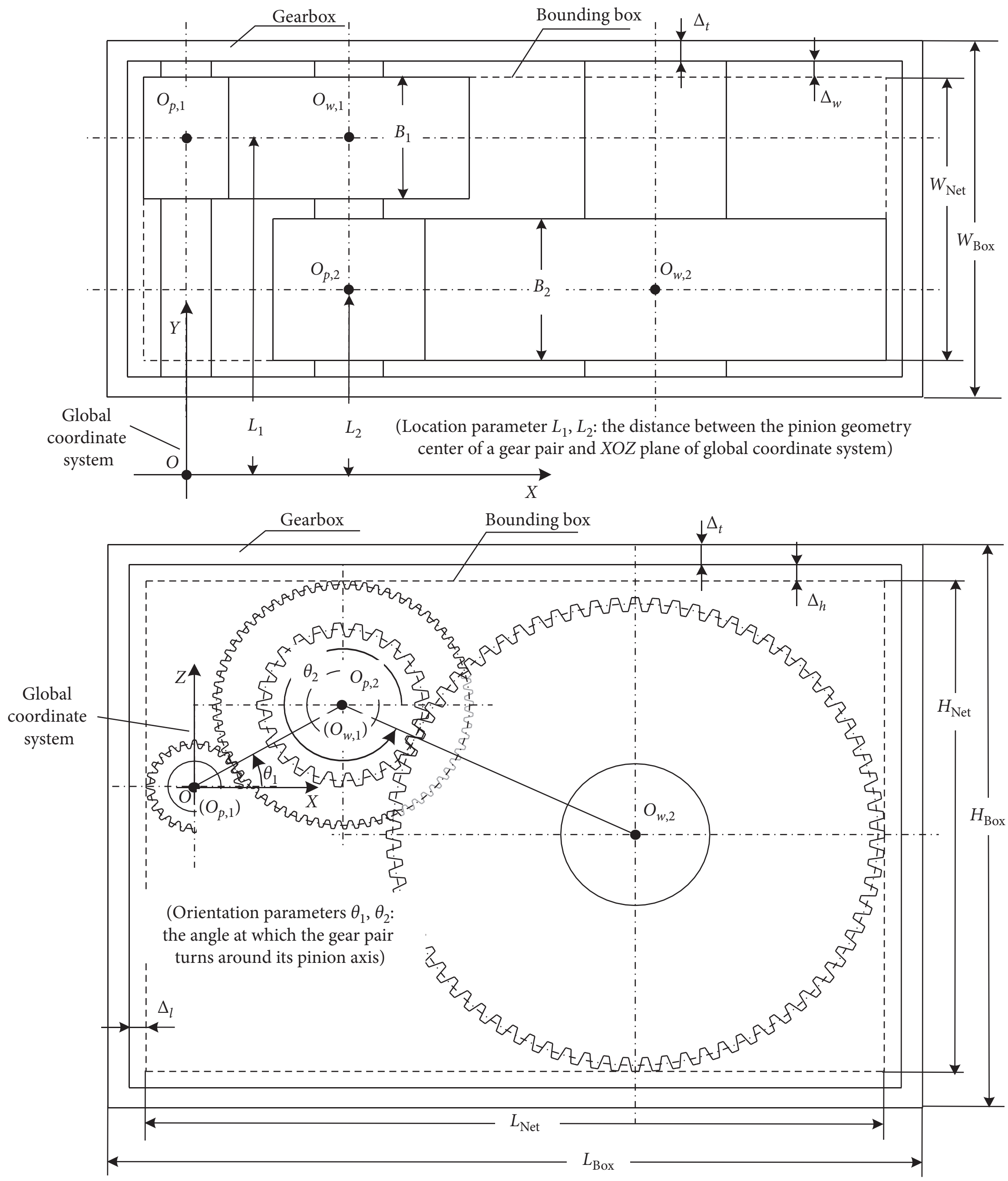

FIGURE 2: Definitions of global coordinate system, layout parameters, gearbox, and bounding box of multistage gear drives with a two-stage gear drive acting as an example.

there will be $8M$ edge-points. According to the character mentioned above, the *left-boundary*, *right-boundary*, *upper-boundary*, and *lower-boundary* of the bounding box of an M-stage gear drive are always tangent to one of the $8M$ edge-points, respectively. For instance, the *left-boundary*, *right-boundary*, *upper-boundary*, and *lower-boundary* to the bounding box of a two-stage gear drive in Figure 3(b) are tangent to the edge-points $P_{1,3}$, $P_{2,5}$, $P_{1,6}$, and $P_{2,8}$, respectively. Then, L_{net} and H_{net} of the bounding box to that two-stage gear drive are $L_{\text{net}} = P_{2,5}^x - P_{1,3}^x$ and $W_{\text{net}} = P_{1,6}^z - P_{2,8}^z$. Here,$P_{1,3}^x$ and $P_{2,5}^x$ are the X-coordinates of $P_{1,3}$ and $P_{2,5}$, respectively, while $P_{1,6}^z$ and $P_{2,8}^z$ are the Z-coordinates of $P_{1,6}$ and $P_{2,8}$, respectively.

Based on above statements, the formula to calculate the L_{net}, W_{net}, and H_{net} of an M-stage gear drive can be expressed by

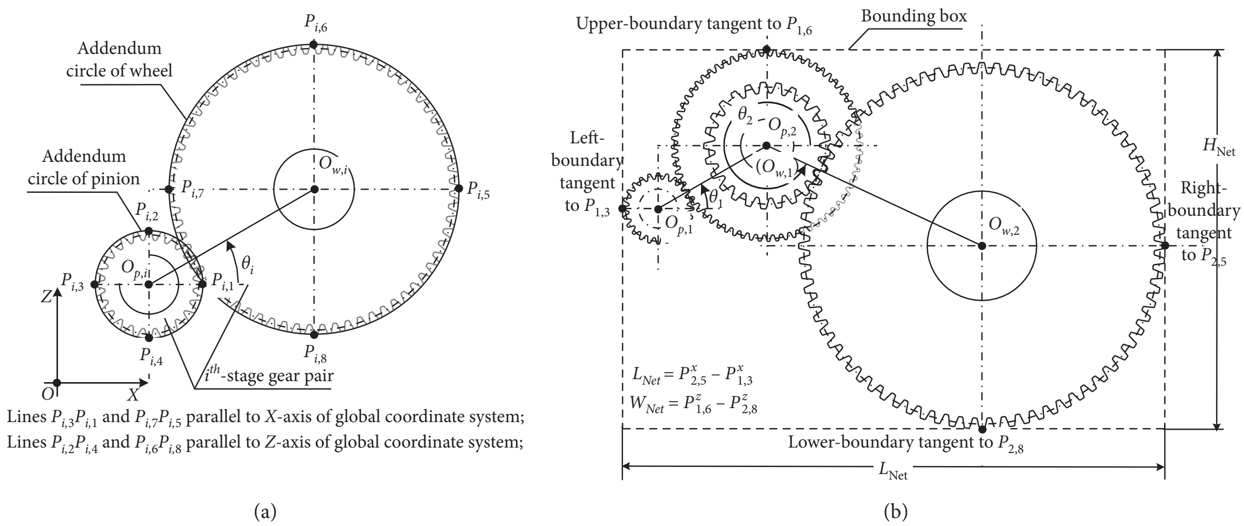

FIGURE 3: (a) Definition of edge-points $P_{i,k}$ ($k = 1, 2, \ldots, 8$) on the addendum circles of i^{th}-stage gear pair. (b) An example of using them to calculate L_{net} and H_{net} of a two-stage gear drive's bounding box.

$$\begin{cases} L_{\text{net}} = \max\left\{P^x_{i,k}\right\} - \min\left\{P^x_{i,k}\right\}, \\ W_{\text{net}} = \max\left\{\dfrac{L_i + B_i}{2}\right\} - \min\left\{\dfrac{L_i - B_i}{2}\right\}, \\ H_{\text{net}} = \max\left\{P^z_{i,k}\right\} - \min\left\{P^z_{i,k}\right\}, \end{cases} \tag{5}$$

$$(i = 1, 2, \ldots, M;\ k = 1, 2, \ldots, 8),$$

where $P^x_{i,k}$ and $P^z_{i,k}$ are the X-coordinate and Z-coordinate of the k^{th}-edge point on i^{th}-stage gear pair $P_{k,i}$, respectively, and

$$P_{i,k} = \begin{cases} O_{p,i} + \left(\cos\dfrac{(k-1)\pi}{2}, 0, \sin\dfrac{(k-1)\pi}{2}\right)\dfrac{d_{pa,i}}{2}, & k = 1, 2, 3, 4, \\ O_{w,i} + \left(\cos\dfrac{(k-4)\pi}{2}, 0, \sin\dfrac{(k-4)\pi}{2}\right)\dfrac{d_{wa,i}}{2}, & k = 5, 6, 7, 8, \end{cases} \tag{6}$$

where $d_{pa,i}$ and $d_{wa,i}$ are the addendum circle diameters of pinion and wheel of i^{th}-stage gear pair, respectively. $O_{p,i}$ and $O_{w,i}$ are the geometry centers of pinion and wheel of i^{th}-stage gear, respectively, and the global coordinates of them can be calculated by

$$\begin{aligned} O_{p,i} &= \begin{cases} (0, L_i, 0), & (i = 1), \\ \left(x_{p,i-1} + a_{i-1}\cos\theta_{i-1}, L_i, z_{p,i-1} + a_{i-1}\sin\theta_{i-1}\right), & i = 2, 3, \ldots, M, \end{cases} \\ O_{w,i} &= \left(x_{p,i} + a_i\cos\theta_i, L_i, z_{p,i} + a_i\sin\theta_i\right), \quad i = 1, 2, \ldots, M, \end{aligned} \tag{7}$$

where a_i is the center distance of i^{th}-stage gear pair, and

$$a_i = \frac{d_{p,i} + d_{w,i}}{2}. \tag{8}$$

2.3. Constraints. In this study, the constraints are divided into three major types: transmission ratio constraint, stress constraint, and interference constraint. The formats of all the constraints' formulas are given by the way of their constraint violations.

2.3.1. Transmission Ratio Constraint. There are two aspects of meanings to the transmission ratio constraint. The first is that the gear ratio of i^{th}-stage gear pair u_i in a gear drive should lie in a proper range $[u_i^l, u_i^u]$, where u_i^l is the lower limit of u_i and u_i^u is the upper limit. This range reveals the ability of how much a specific type of gear pair can reduce the speed transferred through it, and it can be achieved through the design standard employed or by experience. The formulas to this constraint are expressed as

$$\begin{cases} g_{u_i^l}(\vec{x}) = \max(u_i^l - u_i, 0), \\ g_{u_i^u}(\vec{x}) = \max(u_i - u_i^u, 0), \\ u_i = \dfrac{z_{w,i}}{z_{p,i}}, \quad i = 1, 2, \ldots, M, \end{cases} \tag{9}$$

where $g_{u_i^l}(\vec{x})$ and $g_{u_i^u}(\vec{x})$ are the degree of lower-limit and upper-limit constraint violations of u_i, respectively.

The second is that the gearbox ratio of a gear drive calculated by the generated design variables in the optimization process U_{cal} should be equal to the user-defined gearbox ratio U_{def}, or at least within a designated percentage (e.g., 3%). This constraint makes sure that the output speed of a gear drive can satisfy user's desire, and the degree of its constraint violation $g_{u_a}(\vec{x})$ is

$$\begin{cases} g_{u_a}(\vec{x}) = \max\left(\text{abs}\left(\dfrac{1 - U_{\text{cal}}}{U_{\text{def}}}\right) - 0.03, 0\right), \\ U_{\text{cal}} = \displaystyle\prod_{i=1}^{M} u_i. \end{cases} \tag{10}$$

2.3.2. Stress Constraint. When designing a gear pair or shaft, the stress constraints are the most important or basic constraints the designer should keep in mind. Here, the stress constraints of gear pairs refer to the contact strength and bending strength constraint. The formulas used to calculate the constraint violations of them come from the International Standards ISO 6336-2 and ISO 6336-3 (1996) and can be expressed as

$$\begin{cases} g_{\sigma_{H,i}}(\vec{x}) = \max\left(\sigma_{H,i} - \sigma_{HP,i}, 0\right), \\ \sigma_{H,i} = Z_H Z_E Z_\varepsilon Z_\beta \sqrt{\dfrac{F_{t,i}}{B_i d_{p,i}} \dfrac{u_i + 1}{u_i} K_A K_V K_{H\beta} K_{H\alpha}}, \\ \sigma_{\text{HP},i} = \dfrac{\sigma_{H\text{lim}} Z_{\text{NT}} Z_L Z_V Z_R Z_W Z_X}{S_{H\min}}, \quad i = 1, 2, \ldots, M, \end{cases}$$
$$\begin{cases} g_{\sigma_{F,i}}(\vec{x}) = \max\left(\sigma_{F,i} - \sigma_{\text{FP},i}, 0\right), \\ \sigma_{F,i} = \dfrac{F_{t,i}}{B_i m_{n,i}} K_A K_V K_{F\beta} K_{F\alpha} Y_{\text{FS}} Y_\varepsilon Y_\beta, \\ \sigma_{FP,i} = \dfrac{\sigma_{\text{FE}} Y_{\text{ST}} Y_{\text{NT}} Y_{\delta\text{relT}} Y_{R\text{relT}} Y_X}{S_{F\min}}, \quad i = 1, 2, \ldots, M, \end{cases} \tag{11}$$

where $g_{\sigma_{H,i}}(\vec{x})$ and $g_{\sigma_{F,i}}(\vec{x}$ are the degree of contact strength and bending strength constraint violations of the i^{th}-stage gear pair, respectively. The explanations of the factors in above equations are illustrated in *Nomenclature*.

The torsion theory is adopted to approximately estimate the strength of shafts. It is assumed that all the shafts are solid, so the degree of stress constraint violations of them is

$$g_{\tau,j}(\vec{x}) = \max\left(\sqrt[3]{\frac{T_j}{0.2[\tau]}} - d_{sh,j}, 0\right), \quad j = 1, 2, \ldots, M + 1, \tag{12}$$

where T_j is the torque acting in the j^{th} rated shaft cross section, and $[\tau]$ is the allowable stress on the torsion.

2.3.3. Interference Constraint. There are two types of interference constraint, i.e., gear pair interference constraint and shaft interference constraint. A projection method is adopted to check whether two components (gear pair or shaft) in a gear drive interfere with each other. The principle of this method is that when two components interfere with each other, all the projections of them on three coordinate planes have overlap regions [12]. Usually, the (0, 1) method is adopted to evaluate the degree of interference constraint violation (DOICV). This method supposes that when two components interfere with each other, the DOICV is 1; otherwise, it is 0 [13]. However, it should be noticed that the overlap regions under different interference circumstances may not be equal and that makes this method a little inaccurate. Therefore, a more precise method named as projection center distance (PCD) method is proposed. The steps to calculate the DOICV of two components based on PCD method are as follows:

(1) Project the two components on the three two-dimensional coordinate planes, i.e., XOY plane, XOZ plane, and YOZ plane, respectively
(2) Calculate the PCD of two components on each two-dimensional coordinate plane
(3) Calculate the DOICV of two components on each two-dimensional coordinate plane based on their PCD and geometry dimensions
(4) The DOICV of two components in three-dimensional space is the sum of their DOICVs on each two-dimensional coordinate plane

Then, the formulas to calculate the DOICV of gear pair interference constraint and shaft interference constraint based on PCD method are presented below.

(1) Gear Pair Interference Constraint. The gear pair interference constraint refers to the interference between two gear pairs. The interference circumstances of two gear pairs' projections on different coordinate planes are diverse. Nevertheless, they can be assembled by some basic interference types. Figure 4 illustrates the four basic interference types of i^{th}-stage and j^{th}-stage gear pairs' projections on XOZ plane. They are named in turn from (a) to (d) as W^2, WP, P^2, and PW and refer to the interference between the addendum circles of wheel_i and wheel_j, wheel_i and pinion_j, pinion_i and pinion_j, and pinion_i and wheel_j, respectively. Based on these four basic interference types, other kinds of interference types can be assembled. For example, the interference type (W^2, P^2), which means wheel_i and wheel_j, pinion_i and pinion_j interfere with each other simultaneously, is assembled by interference types of W^2 and P^2.

In Figure 4, $d_{ij}^{w^2}$, d_{ij}^{wp}, $d_{ij}^{p^2}$, and d_{ij}^{pw} are the PCDs of the four basic interference types, respectively. The values of them can be calculated by

$$\begin{cases} d_{ij}^{w^2} = \sqrt{\left(O_{w,i}^x - O_{w,j}^x\right)^2 + \left(O_{w,i}^z - O_{w,j}^z\right)^2}, \\ d_{ij}^{wp} = \sqrt{\left(O_{w,i}^x - O_{p,j}^x\right)^2 + \left(O_{w,i}^z - O_{p,j}^z\right)^2}, \\ d_{ij}^{p^2} = \sqrt{\left(O_{p,i}^x - O_{p,j}^x\right)^2 + \left(O_{p,i}^z - O_{p,j}^z\right)^2}, \\ d_{ij}^{pw} = \sqrt{\left(O_{p,i}^x - O_{w,j}^x\right)^2 + \left(O_{p,i}^z - O_{w,j}^z\right)^2}, \\ i = 1, 2, \ldots, M-1;\ j = i+1, i+2, \ldots, M, \end{cases} \tag{13}$$

where $O_{w,i}^x$ ($O_{w,j}^x$) and $O_{w,i}^z$ ($O_{w,j}^z$) are the X-coordinate and Z-coordinate of $O_{w,i}$ ($O_{w,j}$), respectively, while $O_{p,i}^x$ ($O_{p,j}^x$) and $O_{p,i}^z$ ($O_{p,j}^z$) are the X-coordinate and Z-coordinate of $O_{p,i}$ ($O_{p,j}$), respectively.

Let $g_{ij}^{w^2}(\vec{x})$, $g_{ij}^{wp}(\vec{x})$, $g_{ij}^{p^2}(\vec{x})$, and $g_{ij}^{pw}(\vec{x})$ be the DOICVs of the four basic interference types, respectively, and let $g_{xz,ij}^{gg}(\vec{x})$ be the DOICV of i^{th}-stage and j^{th}-stage gear pairs' projections on XOZ plane. Since the real interference circumstances of two gear pairs' projections on XOZ plane can be assembled by the four basic interference types, the value of $g_{xz,ij}^{gg}(\vec{x})$ can be calculated by

$$g_{xz,ij}^{gg}(\vec{x}) = g_{ij}^{w^2}(\vec{x}) + g_{ij}^{wp}(\vec{x}) + g_{ij}^{p^2}(\vec{x}) + g_{ij}^{pw}(\vec{x}), \tag{14}$$

where

$$\begin{cases} g_{ij}^{w^2}(\vec{x}) = \max\left\{\dfrac{d_{wa,i} + d_{wa,j}}{2} + \delta_{xz} - d_{ij}^{w^2}, 0\right\}, \\ g_{ij}^{wp}(\vec{x}) = \max\left\{\dfrac{d_{wa,i} + d_{pa,j}}{2} + \delta_{xz} - d_{ij}^{wp}, 0\right\}, \\ g_{ij}^{p^2}(\vec{x}) = \max\left\{\dfrac{d_{pa,i} + d_{pa,j}}{2} + \delta_{xz} - d_{ij}^{p^2}, 0\right\}, \\ g_{ij}^{pw}(\vec{x}) = \max\left\{\dfrac{d_{pa,i} + d_{wa,j}}{2} + \delta_{xz} - d_{ij}^{pw}, 0\right\}, \\ (i = 1, 2, \ldots, M-1;\ j = i+1, i+2, \ldots, M), \end{cases} \tag{15}$$

where δ_{xz} is the minimal permitted distance between the two gear pairs' projection on XOZ plane. The value of it is set to 10 mm in this study.

Figure 5 illustrates one instance to the interference between two gear pairs' projections on XOY plane. It can be found that the graphs of i^{th}-stage and j^{th}-stage gear pair's projections on XOY plane are rectangles. Here, L_i^{xy} (L_j^{xy}) and W_i^{xy} (W_j^{xy}) are the length and width of the rectangles, respectively, while O_i^{xy} and O_j^{xy} are the geometry centers of the rectangles. Based on the definition of edge-points $P_{i,k}$, the values of L_i^{xy} (L_j^{xy}), W_i^{xy} (W_j^{xy}) and the coordinates of O_i^{xy} and O_j^{xy} are calculated by

$$\begin{cases} O_{x,i}^{xy} = \dfrac{\max\left\{P_{i,k}^x\right\} + \min\left\{P_{i,k}^x\right\}}{2}, \\ O_{y,i}^{xy} = \dfrac{\max\left\{P_{i,k}^y\right\} + \min\left\{P_{i,k}^y\right\}}{2}, \\ (k = 1, 2, \ldots, 8), \end{cases}$$
$$\begin{cases} L_i^{xy} = \max\left\{P_{i,k}^x\right\} - \min\left\{P_{i,k}^x\right\}, \\ W_i^{xy} = B_i, \\ (k = 1, 2, \ldots, 8), \end{cases} \tag{16}$$

where $O_{x,i}^{xy}$ and $O_{y,i}^{xy}$ are the X-coordinate and Y-coordinate of O_i^{xy}, respectively.

In Figure 5, d_x and d_y are the PCDs between O_i^{xy} and O_j^{xy} along the X-axis and Y-axis directions, respectively. The values of them can be calculated by

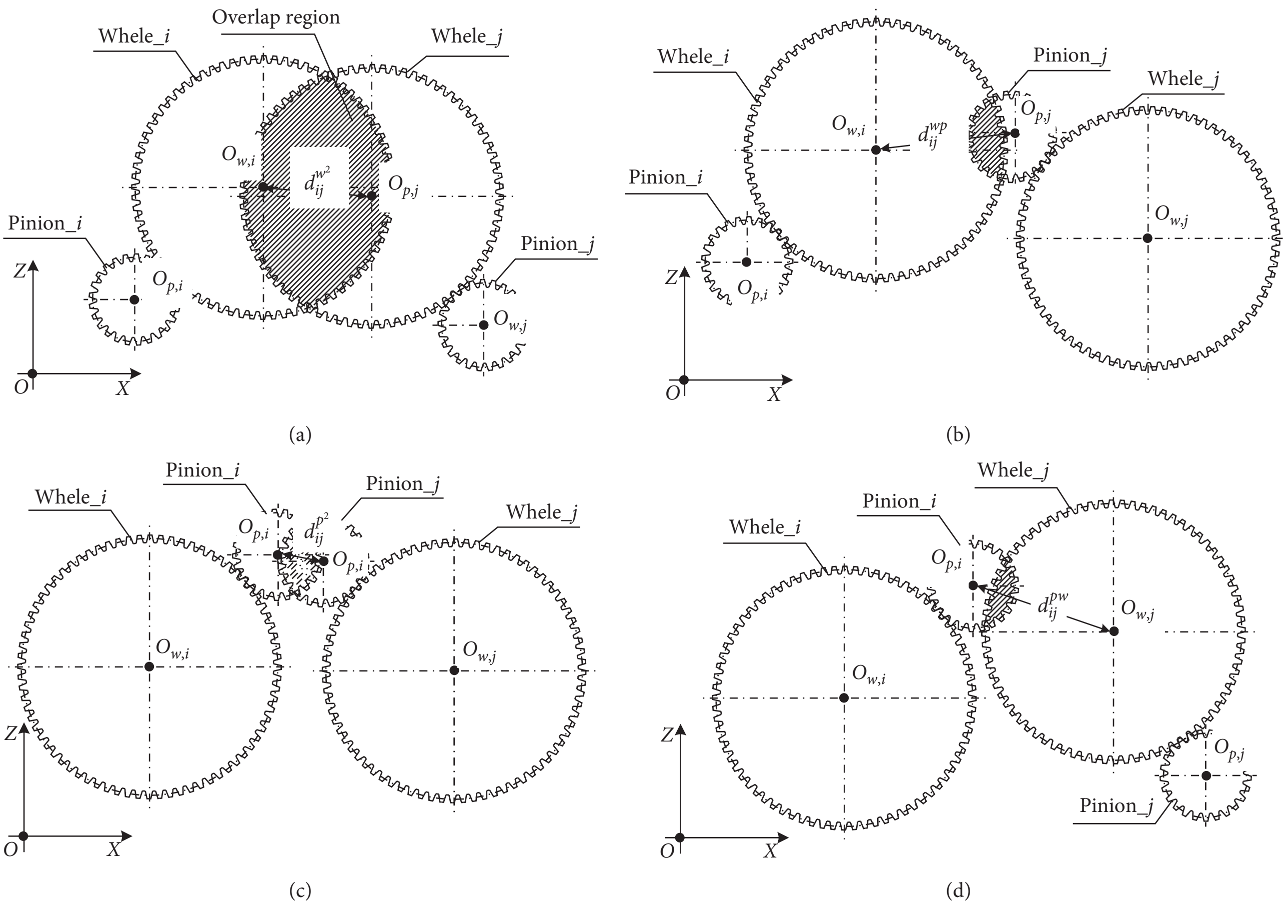

Figure 4: Four basic interference types between the projections of i^{th}-stage and j^{th}-stage gear pairs on XOZ plane.

$$\begin{cases} d_x = abs\left(O_{x,i}^{xy} - O_{x,j}^{xy}\right) \\ d_y = abs\left(O_{y,i}^{xy} - O_{y,j}^{xy}\right) \end{cases}, \quad i = 1, 2, \ldots, M;\ j = 1, 2, \ldots, M;\ i \neq j. \tag{17}$$

When the i^{th}-stage and j^{th}-stage gear pairs' projection on XOY plane interfere with each other, the value of d_x will be smaller than half of the sum of L_i^{xy} and L_j^{xy}, while the value of d_y will be smaller than half of the sum of W_i^{xy} and W_j^{xy} simultaneously. Therefore, the formulas to calculate the DOICV of i^{th}-stage and j^{th}-stage gear pairs' projections on XOY plane, i.e., $g_{xy,ij}^{gg}(\vec{x})$, can be expressed as

$$\begin{cases} \text{if,} & g_{x,ij}(\vec{x}) = d_x - \left[\left(L_i^{xy} + L_j^{xy}\right)/2 + \delta_{xy}\right] \leq 0, \\ \text{and,} & g_{y,ij}(\vec{x}) = d_y - \left[\left(W_i^{xy} + W_j^{xy}\right)/2 + \delta_{xy}\right] \leq 0, \\ & g_{\mathrm{xy,ij}}^{\mathrm{gg}}(\vec{x}) = \mathrm{abs}\left(g_{x,ij}(\vec{x})\right) + abs\left(g_{y,ij}(\vec{x})\right), \\ \text{otherwise,} & g_{\mathrm{xy,ij}}^{\mathrm{gg}}(\vec{x}) = 0, \quad i = 1, 2, \ldots, M-1;\ j = i+1, i+2, \ldots, M, \end{cases} \tag{18}$$

where δ_{xy} is the minimal permitted distance between the two gear pairs' projection on XOY plane, and the value of it is set to 10 mm in this study.

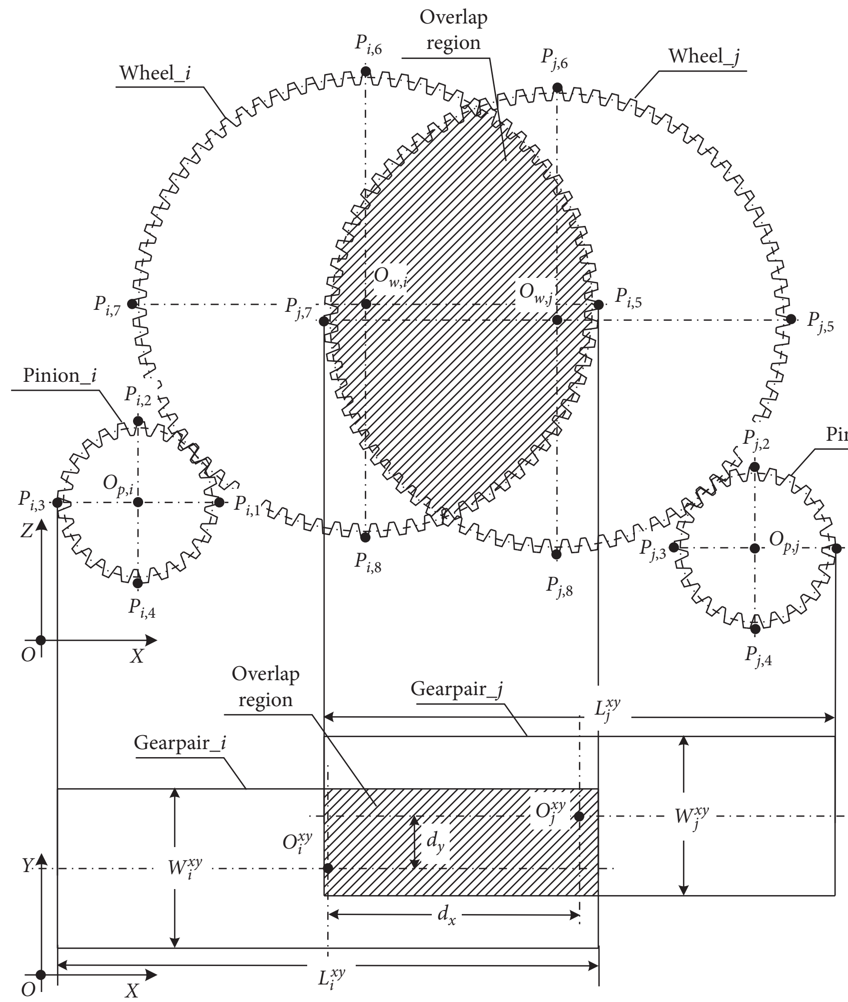

FIGURE 5: The interference between i^{th}-stage and j^{th}-stage gear pairs' projections on XOY plane, an example.

$$\begin{cases} \text{if,} & g^{gg}_{xy,ij}(\vec{x})g^{gg}_{xz,ij}(\vec{x})g^{gg}_{yz,ij}(\vec{x}) \neq 0, \\ & g^{gg}_{ij}(\vec{x}) = g^{gg}_{xy,ij}(\vec{x}) + g^{gg}_{xz,ij}(\vec{x}) + g^{gg}_{yz,ij}(\vec{x}), \\ \text{otherwise,} & g^{gg}_{ij}(\vec{x}) = 0, \quad i = 1,2,\ldots,M-1;\ j = i+1, i+2, \ldots, M. \end{cases} \tag{19}$$

The situation of the interference between two gear pairs' projections on YOZ plane is similar to the situation of XOY plane, so it will not be discussed anymore in this article. Let $g^{gg}_{yz,ij}(\vec{x})$ be the DOICV of two gear pairs' projections on YOZ plane. On the basis of PCD method, the formulas to calculate the DOICV of gear pair interference constraint $g^{gg}_{ij}(\vec{x})$ in three-dimensional space are shown in equation (19).

(2) Shaft Interference Constraint. The shaft interference constraint refers to the interference between a gear pair and a shaft. In this kind of interference, it is only needed to check whether the projections on XOZ plane of a gear pair and a shaft interfere with each other. Similarly, there exist two basic interference types, i.e., WS type and PS type, as shown in Figure 6. Here, $O_{s,j}$ is the projection center of the j^{th} shaft's projection on XOZ plane.

Let d^{ps}_{ij} and d^{ws}_{ij} be the PCD of PS type and WS type, respectively. The values of them can be calculated by

$$\begin{cases} d^{ps}_{ij} = \sqrt{\left(O^x_{p,i} - O^x_{s,j}\right)^2 + \left(O^z_{p,i} - O^z_{s,j}\right)^2}, \\ d^{ws}_{ij} = \sqrt{\left(O^x_{w,i} - O^x_{s,j}\right)^2 + \left(O^z_{w,i} - O^z_{s,j}\right)^2}, \\ i = 1,2,\ldots,M;\ j = 1,2,\ldots,M+1;\ j \neq i;\ j \neq i+1, \end{cases} \tag{20}$$

where $O^x_{s,j}$ and $O^z_{s,j}$ are the X-coordinate and Z-coordinate of $O_{s,j}$, and

$$\begin{cases} O^x_{s,j} = O^x_{p,j}, O^z_{s,j} = O^z_{p,j}, & j = 1,2,\ldots,M, \\ O^x_{s,j} = O^x_{w,j}, O^z_{s,j} = O^z_{w,j}, & j = M+1. \end{cases} \tag{21}$$

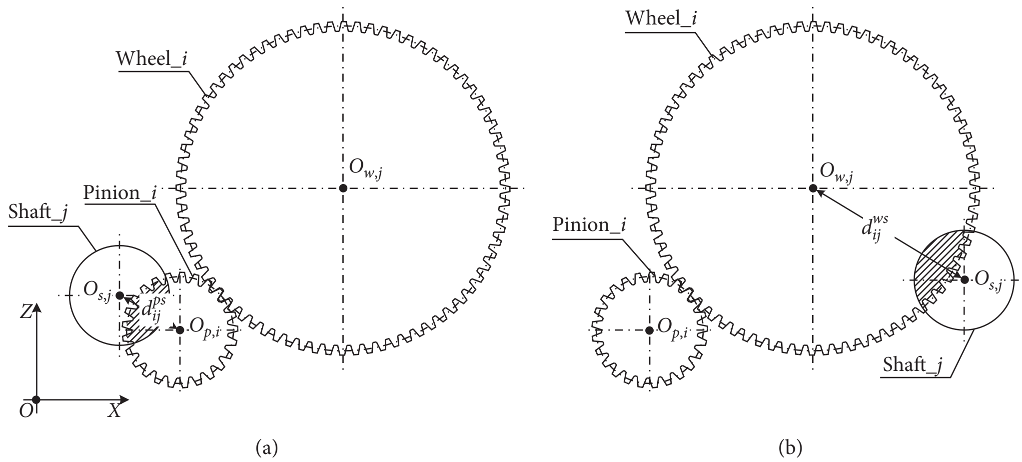

FIGURE 6: Two basic interference types of a shaft and a gear pairs' projections on *XOZ* plane. (a) PS. (b) WS.

Then, the formula to calculate the DOICV of i^{th}-stage gear pair and j^{th} shaft in a gear drive $g_{ij}^{gs}(\vec{x})$ can be expressed as

$$g_{ij}^{gs}(\vec{x}) = g_{ij}^{ps}(\vec{x}) + g_{ij}^{ws}(\vec{x}), \tag{22}$$

where $g_{ij}^{ps}(\vec{x})$ and $g_{ij}^{ws}(\vec{x})$ are the DOICVs of PS type and WS type, respectively, and the values of them can be calculated by

$$\begin{cases} g_{ij}^{ps}(\vec{x}) = \max\left\{\dfrac{d_{pa,i} + d_{sh,j}}{2} + \delta_s - d_{ij}^{ps}, 0\right\}, \\ g_{ij}^{ws}(\vec{x}) = \max\left\{\dfrac{d_{wa,i} + d_{sh,j}}{2} + \delta_s - d_{ij}^{ws}, 0\right\}, \\ (i = 1, 2, \ldots, M;\ j = 1, 2, \ldots, M+1;\ j \neq i;\ j \neq i+1), \end{cases} \tag{23}$$

where δ_s is the minimal permitted distance between the projections of a gear pair and a shaft on *XOZ* plane, and the value of it is set to 10 mm in this study.

3. Specific Comments on the Used Genetic Algorithm

3.1. Algorithm Flow and Genetic Operators. Genetic algorithm (GA) starts with randomly generating an initial population of individuals, and then a self-adaptive iterative search progress is going on generation after generation to find out the optimal solution [14]. In this study, an elitist GA is adopted, and its flowchart is shown in Figure 7(a). The basic character of it is a CombinePop that is formed by combining parent population and offspring population, and then the elitisms are picked up according to a certain probability λ from CombinePop by ExtractPop procedure.

A MATLAB program is developed by Figure 7(a). To make this program adapts to the dimensional and layout optimization problem for any number of stages of cylindrical gear drives, the flowchart of the evaluation procedure is presented in Figure 7(b). Here, Figure 7(b) is a supplementary description of the steps "Evaluate initial population by fitness function" and "Evaluate CombinePop by fitness function" in Figure 7(a). It means that when these two steps are run, the flowchart of Figure 7(b) will be used. In Figure 7(b), M is a positive number that denotes the number of stages of the gear drive. $G(\vec{x})$ is the constraint violation of an individual, and the value of it equals the sum of constraint violations of the constraints presented in Section 2.3. Thus, the formula to calculate it can be expressed by

$$G(\vec{x}) = G_1(\vec{x}) + G_2(\vec{x}) + G_3(\vec{x}) + G_4(\vec{x}) + g_{u_a}(\vec{x}), \tag{24}$$

where

$$\begin{cases} G_1(\vec{x}) = \displaystyle\sum_{i=1}^{M}\left(g_{u_i^l}(\vec{x}) + g_{u_i^u}(\vec{x}) + g_{\sigma_{H,i}}(\vec{x}) + g_{\sigma_{F,i}}(\vec{x})\right), \\ G_2(\vec{x}) = \displaystyle\sum_{j=1}^{M+1} g_{\tau,j}(\vec{x}), \\ G_3(\vec{x}) = \displaystyle\sum_{i=1}^{M-1}\sum_{j=i+1}^{M} g_{ij}^{gg}(\vec{x}), \\ G_4(\vec{x}) = \displaystyle\sum_{i=1}^{M}\sum_{j=1}^{M+1} g_{ij}^{gs}(\vec{x}), \quad j \neq i;\ j \neq i+1. \end{cases} \tag{25}$$

The genetic operators refer to the selection operator, crossover operator, and mutation operator. A wide variety of types to these three operators exists. In this study, the binary tournament selection operator is adopted and proved itself to be working well. The crossover operator and mutation operator adopted are arithmetic crossover operator and Gaussian mutation operator.

3.2. Variables Encoding. The variables encoding is the process to transform the solution space of an actual problem into the searching space of GA. In the running process of

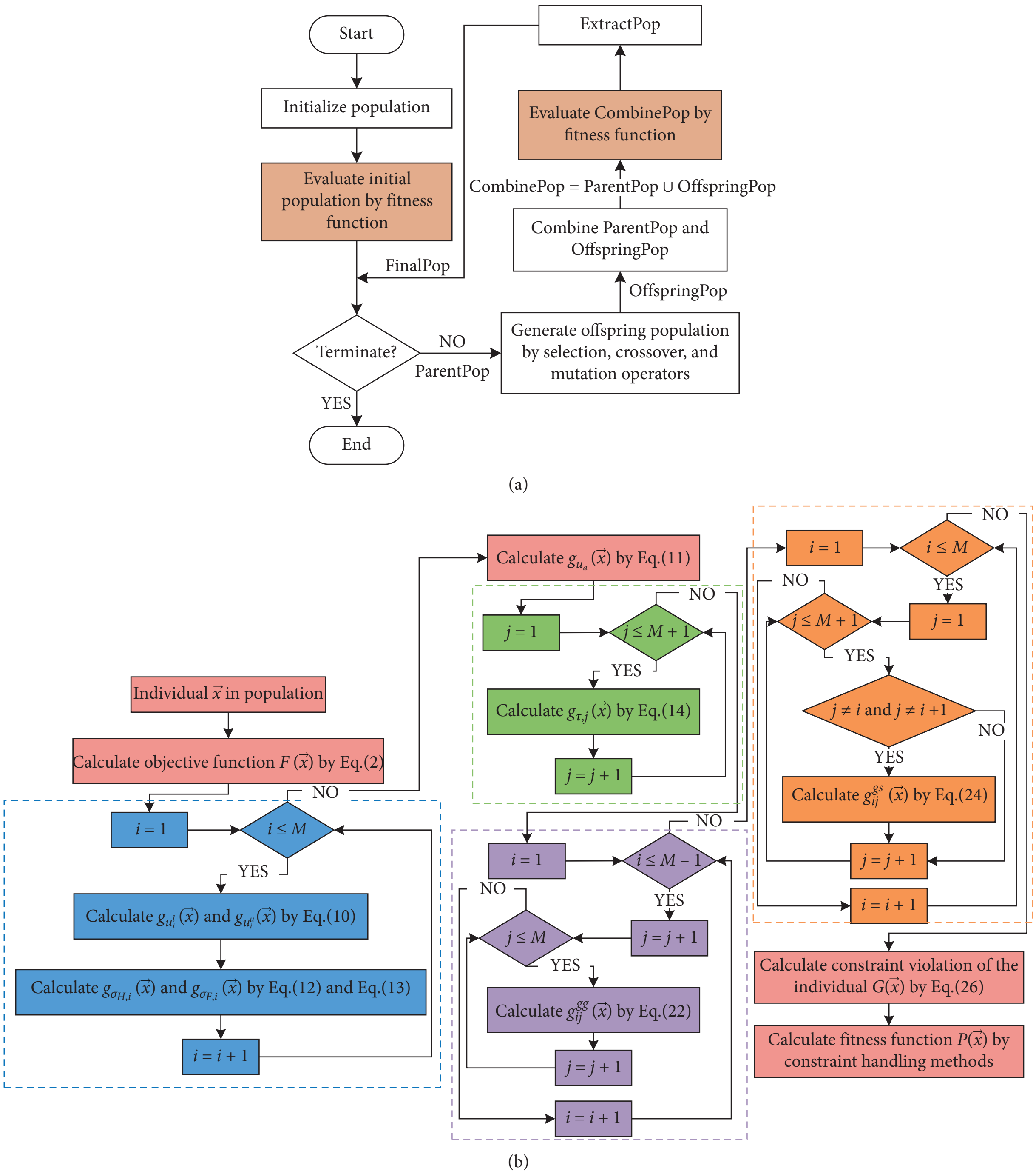

Figure 7: The flowcharts of the used elitist genetic algorithm and its evaluation procedure. (a) The flowchart of the used elitist genetic algorithm. (b) The flowchart of evaluation procedure to each individual.

GA, it does not manipulate the design variables directly, but exerts genetic operations of selection, crossover, and mutation to the genes to realize the aim of optimization [15, 16]. A design variable is usually encoded by one or several genes according to the encoding methods adopted. In this study, a hybrid encoding method for integer-point and float-point is adopted. This method uses an integer number or float number to construct genes. The encoding of design variables $\vec{x}$ (see equation (1)) is illustrated in Table 1 with the range (upper limit and lower limit) of them. Particularly, the type of normal module $m_{n,i}$ is discrete float, and the value of it comes from ISO Standard as set {1, 1.25, 1.5, 2, 2.5, 3, 4, 5, 6, 8} shows.

3.3. Constraint Handling Methods and Fitness Functions. The evolutionary algorithms including GA are essentially unconstrained optimization algorithms. Therefore, when

Table 1: The encoding and range of design variables $\vec{x}$.

Variables	Range	Type
Number of teeth on pinion $z_{p,i}$	[17, 30]	Continuous integer
Number of teeth on wheel $z_{w,i}$	[17, 150]	Continuous integer
Normal module $m_{n,i}$	[1, 8]	Discrete float
Shaft diameter $d_{sh,i}$	[10, 100]	Continuous integer
Face width coefficient Ψ_i	[0.7, 0.85]	Continuous float
Location parameter L_i	[0, 300]	Continuous integer
Orientation parameter θ_i	[0, 360]	Continuous integer

dealing with the constraint optimization problem by GA, the first task is to transform it into unconstraint optimization problem by building up the fitness function to combine the objective function with constraints. Many researchers in the field of computer algorithms have put forward numerous methods to conduct this transformation and construct various types of fitness functions [17–19]. However, when facing up a specific problem, some of these methods may work well, while others may not [20]. This fact gives us an eagerness to figure out which one performs the best in our problem. Thus, three typical constraint handling methods, i.e., static penalty (SP) method [21], the second generation of self-organizing adaptive penalty strategy (SOAPS-II) [22], and an addition of ranking (AR) method [23], are chosen and compared with each other in this study. The formulas to construct the fitness functions based on these methods are presented below.

3.3.1. Static Penalty Method. The static penalty (SP) method is definitely the most classical and popular constraint handling method, for its understanding and implementation simplicity. When applying it in GA to solve our optimization problem, the fitness function $P_{SP}(\vec{x})$ can be expressed by

$$\begin{cases} P_{\mathrm{SP}}(\vec{x}) = F(\vec{x}) + \omega G(\vec{x}), \\ \omega = 2^n, \quad n = -1, 0, 1, 2, \end{cases} \tag{26}$$

where ω is the penalty factor. The performance of SP method mainly depends on the value of ω. For now, the most commonly used values of ω are 2^n and 10^n ($n = -1, 0, 1, 2$). Both of these values have been tested in our optimization problem, and 2^n ($n = -1, 0, 1, 2$) performed better. That is why $\omega = 2^n$ ($n = -1, 0, 1, 2$) is used in SP method to compare with other constraint handling methods.

3.3.2. The Second Generation of Self-Organizing Adaptive Penalty Strategy. The basic character of SOAPS-II is that the values of penalty factors for each constraint are independent and automatically determined according to design population distributions. This is also the biggest difference between SOAPS-II and SP method. The fitness function of SOAPS-II is defined as

$$P_{\mathrm{SOAPS-II}}(\vec{x}, q) = \begin{cases} F(\vec{x}), & \text{if } \vec{x} \text{ is a feasible solution}, \\ F(\vec{x}) \times \left(1 - \dfrac{q}{G_{\max}}\right) + F_{\mathrm{BASE}} \times \dfrac{q}{G_{\max}} + \displaystyle\sum_{j=1}^{\mathrm{N_{const}}} r_j^q \times g_j(\vec{x}, q), & \text{otherwise}, \end{cases} \tag{27}$$

where

$$r_j^q = r_j^{q-1} \times \left[\frac{1 - \left(f_j^q - 0.5\right)}{5}\right], \quad q \geq 1, \tag{28}$$

where F_{BASE} is the minimum objection value of all feasible solutions in the population of q^{th} generation. If there is no feasible solution in that population, F_{BASE} equals objection function value of the solution with the smallest amount of constraint violations. $G_{\max}$ is the number of max generation. r_j^q and f_j^q are the penalty factor and percentage of feasible solutions of j^{th} constraint at the q^{th} generation, respectively. In equation (28), when $q = 0$, the initial value of r_j^q, i.e., r_j^0, can be calculated by

$$r_j^0 = \begin{cases} \dfrac{\mathrm{MID}^1_{\mathrm{obj,feasible},j} - \mathrm{MID}^1_{\mathrm{obj,infeasible},j}}{\mathrm{MID}^1_{\mathrm{con},j}}, & \text{if } \mathrm{MID}^1_{\mathrm{obj,feasible},j} \geq \mathrm{MID}^1_{\mathrm{obj,infeasible},j}, \\ \dfrac{0.5 \times \left(\mathrm{MID}^1_{\mathrm{obj,infeasible},j} - \mathrm{MID}^1_{\mathrm{obj,feasible},j}\right)}{\mathrm{MID}^1_{con,j}}, & \text{otherwise}, \end{cases} \tag{29}$$

where $\mathrm{MID}^1_{\mathrm{obj,feasible},j}$ and $\mathrm{MID}^1_{\mathrm{obj,infeasible},j}$ are the median of the objective function values of all solutions in the initial population which are feasible and infeasible to the j^{th} constraint, respectively. $\mathrm{MID}^1_{\mathrm{cons},j}$ is the median of all constraint violations to the j^{th} constraint in the initial population.

3.3.3. An Addition of Ranking Method. Differing from the SP method and SOAPS-II, the addition of ranking (AR) method takes not only the value of objective function $F(\vec{x})$ and the degree of constraint violation of an individual into consideration to construct the fitness function, but also the number of constraints that are not satisfied. It ranks the individuals with respect to these three terms independently. The ranking numbers of them are represented by R_f, R_s, and R_v, respectively. Clearly, R_f, R_s, and R_v are in the same order of magnitude, and each ranges from 1 to N_{pop} (the size of population). Considering the different distributions of feasible and infeasible individuals in the population, the fitness function of AR method is

$$P_{\text{AR}}(\vec{x}) = \begin{cases} R_s + R_v, & \text{if all the individuals in the population are infeasible,} \\ R_f + R_s + R_v, & \text{otherwise.} \end{cases} \quad (30)$$

4. Design Example

In this section, the proposed optimization model is applied to the dimensional and layout optimization design of an existing three-stage external spur gear drive. Through this design example, the applicability of the proposed optimization model will be tested. Meanwhile, the SP, SOAPS-II, and AR constraint handling methods will be applied in GA one by one to test their performance on the optimization problem. The comparison between the proposed PCD method and (0, 1) method to calculate the DOICV will be conducted and presented.

4.1. Design Specifications and Dimension and Layout of Existing Gear Drive. Table 2 shows the design specifications of the existing three-stage external spur gear drive. These specifications will also be used in the optimization design procedure. According to the design specifications, the gear pairs and shafts of the existing gear drive were designed by the conventional trial and error methods presented in Springer Handbook of Mechanical Engineering [24]. The dimensional parameters of the existing gear drive are illustrated in Table 3. The layout of the existing gear drive is shown in Figure 8. It is a kind of expanded layout style and does not take the effect of orientation parameter on the volume of bounding box into consideration.

4.2. Optimization Results and Discussion. In the dimensional and layout optimization problem of the three-stage gear drive, nine different test cases were done by applying three different constraint handling methods (i.e., SP, SOAPS, and RM methods) and two different calculation methods of DOICV (i.e., (0,1) method and PCD method) in GA, respectively. To each type of test cases, GA was run with the same values of design specifications (see Table 2). Meanwhile, the population size and max generation were fixed to $10N_{\text{var}} = 220$ and 800, respectively, and the crossover and mutation rate were fixed to 0.7 and 0.1, respectively. The proportion of elitisms λ was fixed to 0.2. Since GA is a stochastic method, its results have to be analyzed in terms of repeatability. So, for each type of test cases, the GA has been run 30 times repeatedly.

The obtained optimization results of the nine test cases are summarized and presented in Table 4. In that table, the first column lists the names (from *Case* 1 to *Case* 9) of the nine test cases. The number of *infeasible* solutions column lists the number of runs out of 30 repeat GA runs that cannot find a feasible solution in the final generation. The *Best*, *Average*, and *Worst* columns list the minimum, average, and maximum objective function values within the feasible optimization solutions found by 30 repeat GA runs for each test case, respectively.

As shown in the rows *Case* 1 to *Case* 4 of Table 4, four different penalty factors, i.e., $\omega = 2^{-1}, 2^0, 2^1, 2^2$, for SP constraint handling methods with PCD method to calculate the DOICV were tested. When $\omega = 2^{-1}$ (*Case* 1), no feasible solution was found out of 30 GA runs. As for the other three cases, i.e., *Case* 2 to *Case* 4, all of them can find a feasible solution in the final generation of each GA run. Yet, after comparing the values of *Best*, *Average*, and *Worst* columns of these three cases, $\omega = 2^0$ (*Case* 1) performed the best. Comparing the *Best*, *Average*, and *Worst* columns of *Case* 6 and *Case* 8 with *Case* 4, it is clearly that *Case* 6 and *Case* 8 consistently discover better final designs than *Case* 4. Besides, *Case* 8 has the best performance in every item being compared. Similarly, comparing the same items of *Case* 9 with *Case* 5 and *Case* 7, *Case* 9 also performed the best in these three cases. Since the RM constraint handling method was adopted in test cases *Case* 8 and *Case* 9, it is believed that the RM constraint handing method is better than the other twos in handling the constraints in the optimization problem tested.

In the test cases *Case* 4, *Case* 6, and *Case* 8, the (0, 1) method was used to calculate the DOICV with SP ($\omega = 2^0$), while SOAPS-II and RM methods were used to handle the constraints, respectively. In the test cases *Case* 5, *Case* 7, and *Case* 9, the proposed PCD method was used to calculate the DOICV with SP ($\omega = 2^0$), while SOAPS-II and RM methods were used to handle the constraints, respectively. Figure 9 shows the convergence histories of these six test cases. In that figure, the vertical axis represents the minimum objective function values of the feasible solutions at any given generation from the corresponding 30 repeat GA runs. At the end of 800 generations, these values will be actually identical to the corresponding values under the *Best*, *Average*, and *Worst* columns of Table 4. As shown in Figure 9, the convergence curves of PCD methods produced a more effective convergence history than the corresponding convergence

Table 2: Design specifications.

Parameters	Value
Transmitted power (kW)	10
Input speed (rpm)	960
Gearbox ratio	25
Lower limit of gear ratio u_i^l	1
Upper limit of gear ratio u_i^u	5
Number of stages	3
Pressure angle (degree)	20
Application factor K_A	1.25
Gear material	20CrMnTi
Heat treatment of gear material	Carburized and case-hardened
Hardness of gear material (HRC)	56~62
Shaft material	45 steel
Heat treatment of shaft material	Tempering treatment
Bending stress limit σ_{Flim} (MPa)	460
Contact stress limit σ_{Hlim} (MPa)	1500
Minimum safety factor for bending S_{Flim}	1.25
Minimum safety factor for contact S_{Hlim}	1.1
Allowable torsional stress of shaft $[\tau]$ (MPa)	35

Table 3: Parameters of the existing gear drive.

Stage	Teeth number ($z_{p,i}$, $z_{w,i}$)		Gear ratio u_i	Module $m_{n,i}$ (mm)	Face width coefficient Ψ_i	Helical angle β_i (degree)	Face width B_i (mm)		Shaft diameter $d_{sh,j}$ (mm)	
1st	$z_{p,1}$	22	2.6818	2	0.7319	12.6015	B_1	33	$d_{sh,1}$	26
	$z_{w,1}$	59								
2nd	$z_{p,2}$	20	3.6000	3	0.7289	13.6316	B_2	45	$d_{sh,2}$	36
	$z_{w,2}$	72							$d_{sh,3}$	55
3rd	$z_{p,3}$	22	2.6364	4	0.7206	12.6804	B_3	65	$d_{sh,4}$	75
	$z_{w,3}$	58								

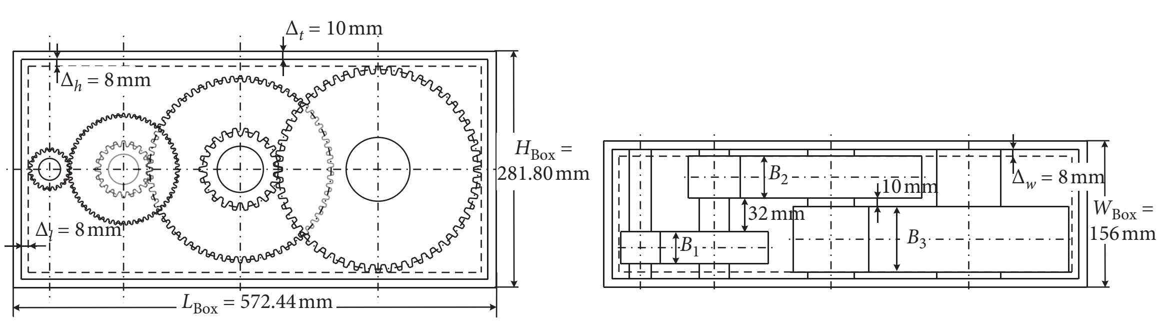

Figure 8: The layout of the existing three-stage external spur gear drive.

Table 4: The optimization results out of 30 repeat GA runs for each test case.

Test cases	Constraint handling methods	Calculation methods of DOICV	Number of *infeasible* solutions	Optimized objective function $F(\vec{x})$ ($\times 10^6$ mm^3)		
				Best	*Average*	*Worst*
Case 1	SP ($\omega = 2^{-1}$)	PCD	30			
Case 2	SP ($\omega = 2^{1}$)	PCD	0	8.2487	8.4801	8.6830
Case 3	SP ($\omega = 2^{2}$)	PCD	0	8.2370	8.4344	8.5844
Case 4	SP ($\omega = 2^{0}$)	PCD	1	**8.1950**	8.4042	8.5682
Case 5	SP ($\omega = 2^{0}$)	(0, 1)	1	8.2416	8.4246	8.5962
Case 6	SOAPS-II	PCD	0	**8.1637**	8.3321	8.4196
Case 7	SOAPS-II	(0, 1)	0	8.2159	8.4079	8.5318
Case 8	RM	PCD	0	**7.9015**	8.1276	8.2859
Case 9	RM	(0, 1)	0	7.9987	8.1552	8.3195

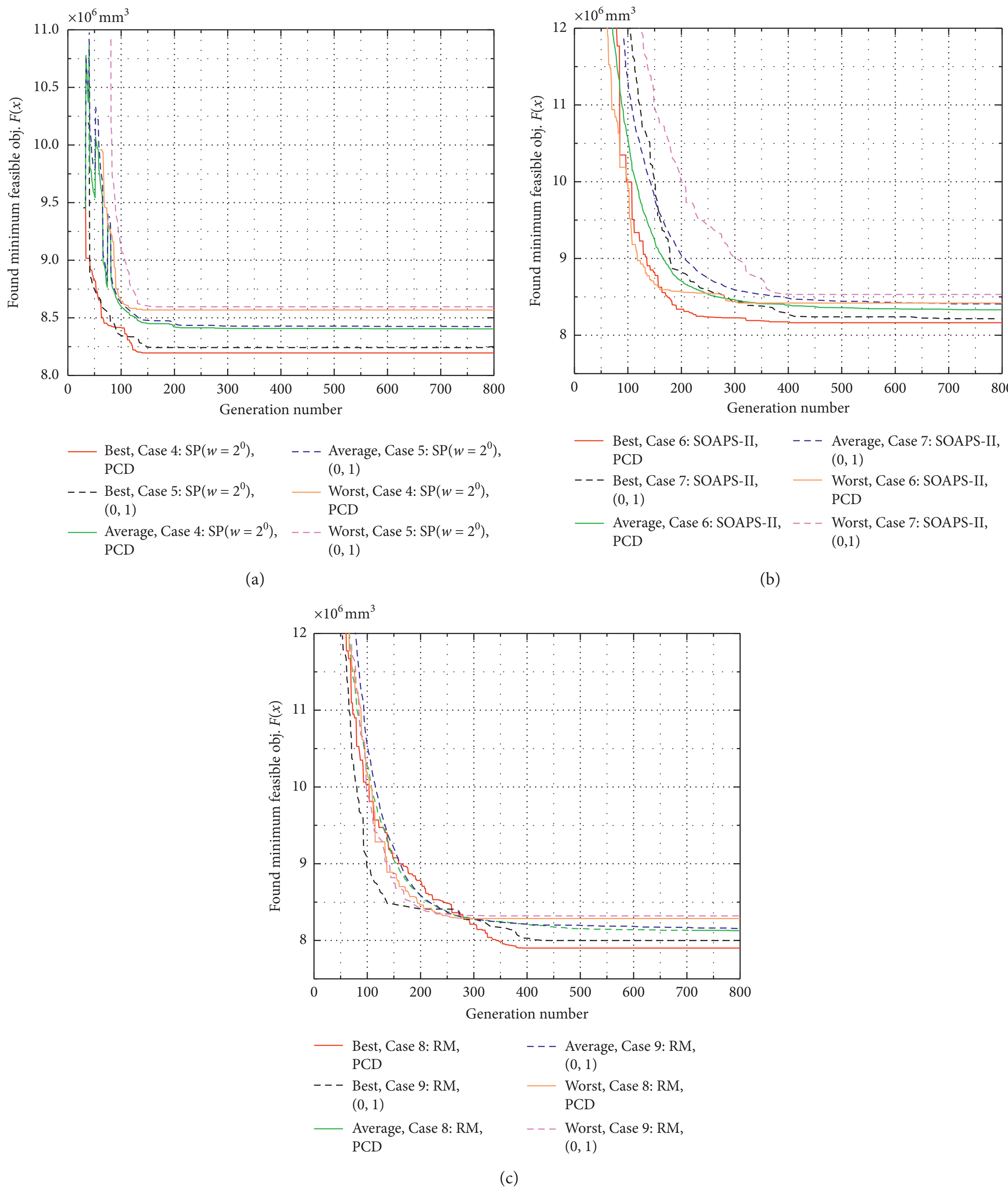

Figure 9: The *Best*, *Average*, and *Worst* convergence histories of *Case* 4 to *Case* 9. (a) Convergence histories of *Case* 4 and *Case* 5. (b) Convergence histories of *Case* 6 and *Case* 7. (c) Convergence histories of *Case* 8 and *Case* 9.

curves of (0, 1) methods among all cases. Furthermore, the values of *Best*, *Average*, and *Worst* of *Case* 4, *Case* 6, and *Case* 8 are all smaller than those of *Case* 5, *Case* 7, and *Case* 9, respectively in Table 4. Thus, it is believed that the paper's proposed PCD method is better than the (0, 1) method to calculate the DOICV in the optimization problem.

Table 5 illustrates the optimized dimensional and layout parameters to the *Best* solutions of *Case* 4, *Case* 6, and *Case* 8. These three optimized solutions are the best-found solutions in runs where SP, SOAPS-II, and RM methods were applied in GA, respectively. Based on their optimized parameters, the layout and size of gearbox of them are presented in Figure 10. Since the *Best* solution of *Case* 8 has the smallest

Table 5: Optimized dimensional and layout parameters to the *Best* solutions found by *Case* 4, *Case* 6, and *Case* 8.

Optimized solutions	Stage	Teeth number ($z_{p,i}$, $z_{w,i}$)		Module $m_{n,i}$ (mm)	Face width coefficient Ψ_i	Location para-meter L_i (mm)	Orientation para-meter θ_i (degree)	Shaft diameter $d_{sh,j}$ (mm)	
Best of Case 4: SP ($\omega = 2^0$), PCD method	1st	$z_{p,1}$	27	1.5	0.7072	118	162	$d_{sh,1}$	25
		$z_{w,1}$	60					$d_{sh,2}$	32
	2nd	$z_{p,2}$	20	2.5	0.7006	69	65	$d_{sh,3}$	50
		$z_{w,2}$	76						
	3rd	$z_{p,3}$	25	3	0.7170	125	342	$d_{sh,4}$	75
		$z_{w,3}$	72						
Best of Case 6: SOAPS-II, PCD method	1st	$z_{p,1}$	25	1.5	0.7316	95	209	$d_{sh,1}$	25
		$z_{w,1}$	66					$d_{sh,2}$	34
	2nd	$z_{p,2}$	26	2	0.7004	139	99	$d_{sh,3}$	50
		$z_{w,2}$	82						
	3rd	$z_{p,3}$	19	4	0.7008	83	194	$d_{sh,4}$	75
		$z_{w,3}$	56						
***Best** of Case* 8: RM, PCD method (the optimal one)	1st	$z_{p,1}$	21	2	0.7022	90	156	$d_{sh,1}$	25
		$z_{w,1}$	49					$d_{sh,2}$	33
	2nd	$z_{p,2}$	20	2.5	0.7000	145	71	$d_{sh,3}$	49
		$z_{w,2}$	65						
	3rd	$z_{p,3}$	24	3	0.7087	91	347	$d_{sh,4}$	75
		$z_{w,3}$	77						

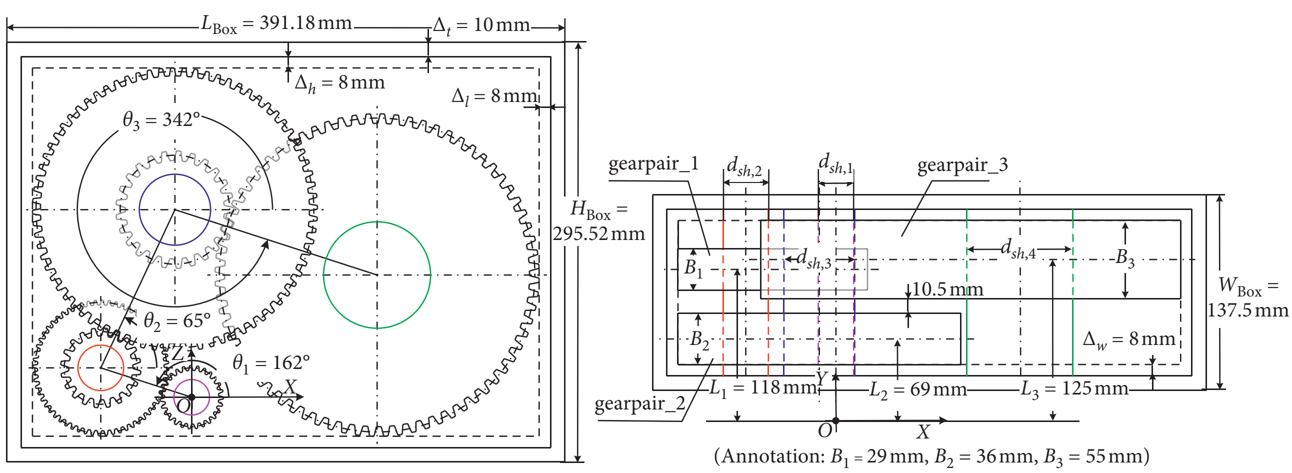

(a)

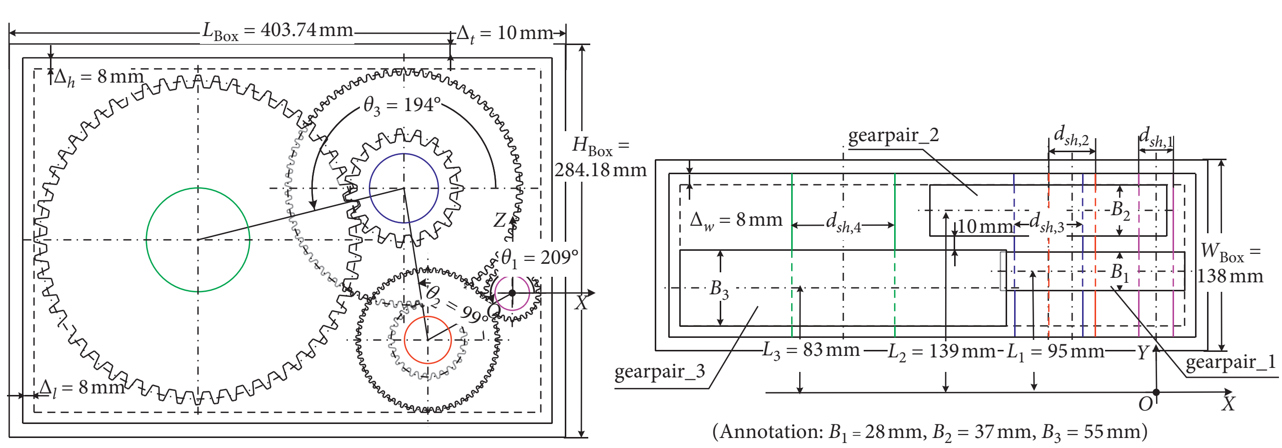

(b)

Figure 10: Continued.

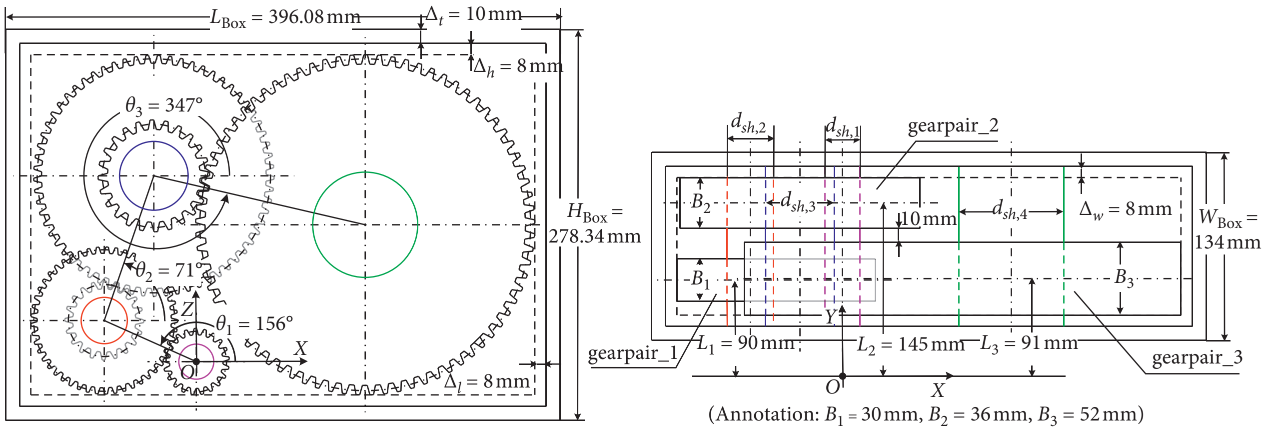

(c)

FIGURE 10: The layout and size of gearbox to the *Best* solutions of *Case* 4, *Case* 6, and *Case* 8. (a) The layout for the *Best* solution of *Case* 4. (b) The layout for the *Best* solution of *Case* 6. (c) The layout for the *Best* solution of *Case* 8, the optimal one.

TABLE 6: Comparison of the volumes between the existing gear drive and the *Best* solutions of *Case* 4, *Case* 6, and *Case* 8.

Volume items	Existing gear drive	*Best* of *Case* 4		*Best* of *Case* 6		*Best* of *Case* 8	
		Volume	Reduced ratio (%)	Volume	Reduced ratio (%)	Volume	Reduced ratio (%)
$\sum_{i=1}^{3} V_{\text{gearpair},i}$ ($\times 10^6$ mm^3)	4.9692	3.2607	34.4	3.2191	35.2	3.1795	36.0
$\sum_{j=1}^{4} V_{\text{shaft},j}$ ($\times 10^6$ mm^3)	1.3014	1.0555	18.9	1.0737	17.5	1.0251	21.2
V_{GearBox} ($\times 10^6$ mm^3)	5.4954	3.8787	29.4	3.8710	29.6	3.6970	32.7
$F(\vec{x})$ ($\times 10^6$ mm^3)	11.7660	8.1950	30.4	8.1637	30.6	7.9015	32.8

optimized value of objective function $F(\vec{x})$, it is identified as the optimal solution in all the test cases of the optimization problem. Table 6 illustrates the comparison results of the volumes between the existing gear drive and the *Best* solutions of *Case* 4, *Case* 6, and *Case* 8. Four different volume items of the gear drive were compared, and they are the sum of volume of gear pairs $\sum_{i=1}^{3} V_{\text{gearpair},i}$, the sum of shaft volumes $\sum_{j=1}^{3} V_{\text{shaft},j}$, the volume of gearbox V_{GearBox}, and the volume of optimized objective function $F(\vec{x})$. The comparison results show that all four volume items to the three *Best* solutions were reduced compared with the existing gear drive. It reveals that the proposed optimization model does realize the object of optimizing the dimensional and layout parameters of multistage cylindrical gear drive simultaneously.

5. Conclusions

This paper proposed a new optimization model that can carry out the dimensional and layout optimization design for any series of cylindrical gear drives simultaneously. To verify the applicability of this model, it has been applied to the dimensional and layout optimization problem of an existing three-stage gear drive solved by an elitism GA. A comparative analysis to the results obtained by GA has been given and the conclusions can be summarized as follows:

(1) The proposed model has been proved to be able to optimize the dimensional and layout parameters of the existing three-stage spur gear drive simultaneously. The comparison of the volumes of the obtained optimized solutions and the existing gear drive has been conducted. The results show that the volumes of the gear pairs, shafts, and gearbox as well as the overall volume have been reduced dramatically compared with the existing gear drive.

(2) Three typical constraint handling methods, i.e., the static penalty (SP) method, the second generation of self-organizing adaptive penalty strategy (SOAPS-II), and an addition of ranking (AR) method, have been applied in GA one by one to deal with the constraints in the optimization problem. For each of them, GA has been run 30 repeat times with the same design specifications and coefficients. The obtained results of them have been summarized in terms of *Infeasible* and the *Best*, *Average*, and *Worst* values of the optimized objective function. After comparing the values of these terms, it is believed that AR method performs the best and finds the optimal solution.

(3) Considering the fact that the overlap regions under different interference situations between two components (i.e., two gear pairs or a gear pair and shaft) may not be equal, the paper proposed a projection center distance (PCD) method to calculation the degree of interference constraint violation (DOICV). After comparing the results of it with the results of (0, 1) method, the PCD method is proved to be able to find better solutions.

Nomenclature

σ_H, σ_{HP}: Calculated and permissible contact stress
σ_F, σ_{FP}: Calculated and permissible bending stress
σ_{Hlim}: Allowable contact and bending stress
σ_{Flim}: Allowable contact and bending stress
F_t: Nominal tangential load
Z_H: Zone factor
Z_E: Elasticity factor
Z_ε: Contact ratio factor for contact stress
Z_β: Helix angle factor for contact stress
K_A: Application factor
K_V: Dynamic factor
$K_{H\beta}$: Face load factor for contact stress
$K_{F\beta}$: Face load factor for bending stress
$K_{H\alpha}$: Transverse load factor for contact stress
$K_{F\alpha}$: Transverse load factor for bending stress
Y_{FS}: Composite tooth shape factor
Y_ε: Contact ratio factor for bending stress
Y_β: Helix angle factor for bending stress
Z_{NT}, Y_{NT}: Life factor for contact and bending stress
Z_X, Y_X: Size factor for contact and bending stress
Z_L: Lubricant, factor for contact stress
Z_V: Velocity factor for contact stress
Z_R: Roughness factor for contact stress
Z_W: Work hardening factor
Y_{ST}: Stress correction factor
$Y_{\delta\mathrm{relT}}$: Relative notch sensitivity factor
$Y_{R\mathrm{relT}}$: Relative surface factor
$S_{H\min}$: Minimum required safety factor for contact stress
$S_{F\min}$: Minimum required safety factor for contact stress.

Data Availability

The data used to support the findings of this study are available from the corresponding author upon request.

Conflicts of Interest

The authors declare that they have no conflicts of interest regarding the publication of this paper.

Acknowledgments

This paper was supported by the State Key Program of the National Natural Science Foundation of China (Grant no. 51535009) and 111 Project of China (Grant no. B13044).

References

[1] I. Bae, T. H. Chong, and A. Kubo, "Development and application of an automatic design system for multi-stage gear drives," in *Proceedings of the ASME 2003 Design Engineering Technical Conferences and Computers and Information in Engineering Conference*, Chicago, IL, USA, September 2003.

[2] N. Marjanovic, B. Isailovic, V. Marjanovic, Z. Milojevic, M. Blagojevic, and M. Bojic, "A practical approach to the optimization of gear trains with spur gears," *Mechanism and Machine Theory*, vol. 53, pp. 1–16, 2012.

[3] C. Gologlu and M. Zeyveli, "A genetic approach to automate preliminary design of gear drives," *Computer & Industrial Engineering*, vol. 57, no. 3, pp. 1043–1051, 2009.

[4] A. Swantner and M. I. Campbell, "Topological and parametric optimization of gear trains," *Engineering Optimization*, vol. 44, no. 11, pp. 1351–1368, 2012.

[5] R. T. Marler and J. S. Arora, "Survey of multi-objective optimization methods for engineering," *Structural and Multidisciplinary Optimization*, vol. 26, no. 6, pp. 369–395, 2004.

[6] S. Padmanabhan, V. S. Raman, and M. Chandrasekaran, "Optimisation of gear reducer using evolutionary algorithm," *Materials Research Innovations*, vol. 18, no. sup6, pp. 378–383, 2014.

[7] T. Yokota, T. Tagughi, and M. Gen, "A solution method for optimal weight design problem of the gear using genetic algorithms," *Computers & Industrial Engineering*, vol. 35, no. 3-4, pp. 523–526, 1998.

[8] V. Savsani, R. V. Rao, and D. P. Vakharia, "Optimal weight design of a gear train using particle swarm optimization and simulated annealing algorithms," *Mechanism and Machine Theory*, vol. 45, no. 3, pp. 531–541, 2010.

[9] F. Mendi, T. Baskal, K. Boran, and F. E. Boran, "Optimization of module, shaft diameter and rolling bearing for spur gear through genetic algorithm," *Expert Systems with Applications*, vol. 37, no. 12, pp. 8058–8064, 2010.

[10] S. Golabi, J. J. Fesharaki, and M. Yazdipoor, "Gear train optimization based on minimum volume/weight design," *Mechanism and Machine Theory*, vol. 73, pp. 197–217, 2014.

[11] T. H. Chong, I. Bae, and G.-J. Park, "A new and generalized methodology to design multi-stage gear drives by integrating the dimensional and the configuration design process," *Mechanism and Machine Theory*, vol. 37, no. 3, pp. 295–310, 2002.

[12] X. Y. Wang, Y. S. Wang, and A. H. B. Duffy, "Spatial layouts of complex mechanical systems," in *Proceedings of the ASME 2005 International Design Engineering Technical Conferences & Computers and Information in Engineering Conference*, Long Beach, CA, USA, September 2005.

[13] J. Bénabès, E. Poirson, F. Bennis, and Y. Ravaut, "Perceptive exploration of layout designs using an interactive genetic algorithm," in *Proceedings of the ASME 11th Biennial Conference on Engineering Systems Design and Analysis*, Nantes, France, 2012.

[14] D. Coit, *Genetic Algorithms and Engineering Design*, John Wiley & Sons, New York, NY, USA, 1997.

[15] J. L. Marcelin, "Using genetic algorithms for the optimization of mechanisms," *International Journal of Advanced Manufacturing Technology*, vol. 27, pp. 2–6, 2005.

[16] X. H. Luo, R. H. Zhang, and K. Cao, "An improved genetic algorithm and its application in optimization design of the gear transmissions," *Machine Design & Research*, vol. 22, pp. 64–67, 2006.

[17] E. Juárez-Castillo, N. Pérez-Castro, and E. Mezura-Montes, "A novel boundary constraint handling technique for constrained numerical optimization problems," in *Proceedings of the 2015 IEEE Congress on Evolutionary Computation (CEC)*, Sendai, Japan, May 2015.

[18] C. J. Zhang, Y. Wu, L. Gao et al., "A new constraint handling method for differential evolution solving non-convex economic dispatch problems with valve loading effect," in *2016 IEEE Congress on Evolutionary Computation (CEC)*, Vancouver, Canada, July 2016.

[19] H. B. Zhang and G. P. Rangaiah, "An efficient constraint handling method with integrated differential evolution for numerical and engineering optimization," *Computers and Chemical Engineering*, vol. 37, pp. 74–88, 2012.
[20] A. Ponsich, C. A. Pantel, S. Domenech, and L. Pibouleau, "Constraint handling strategies in genetic algorithms application to optimal batch plant design," *Chemical Engineering and Processing: Process Intensification*, vol. 47, no. 3, pp. 420–434, 2008.
[21] A. Homaifar, C. X. Qi, and S. H. Lai, "Constrained optimization via genetic algorithms," *Simulation Transactions of the Society for Modeling & Simulation International*, vol. 62, pp. 242–253, 1994.
[22] W. H. Wu and C. Y. Lin, "The second generation of self-organizing adaptive penalty strategy for constrained genetic search," *Advances in Engineering Software*, vol. 35, no. 12, pp. 815–825, 2004.
[23] P. Y. Ho and K. Shimizu, "Evolutionary constrained optimization using an addition of ranking method and a percentage-based tolerance value adjustment scheme," *Information Sciences*, vol. 177, no. 14, pp. 2985–3004, 2007.
[24] K. H. Grote and E. K. Antonsson, *Springer Handbook of Mechanical Engineering*, Springer, Berlin, Germany, 2009.